Applied Mathematics and Computation 270 (2015) 358–368

Contents lists available at ScienceDirect

Applied Mathematics and Computation

journal homepage: www.elsevier.com/locate/amc

Adjoint method for a tumor invasion PDE-constrained optimization problem in 2D using adaptive finite element method

A.A.I. Quiroga, D. Fernández*, G.A. Torres, C.V. Turner

Facultad de Matemática, Astronomía y Física, CIEM–CONICET, Av. Medina Allende s/n, X5000HUA Córdoba, Argentina

ARTICLE INFO

Keywords:
Reaction–diffusion 2D equation
Tumor invasion
PDE-constrained optimization
Adjoint method
Adaptive finite element method
Splitting method

ABSTRACT

In this paper we present a method for estimating an unknown parameter that appears in a two dimensional non-linear reaction–diffusion model of cancer invasion. This model considers that tumor-induced alteration of micro-environmental pH provides a mechanism for cancer invasion. A coupled system reaction–diffusion describing this model is given by three partial differential equations for the 2D non-dimensional spatial distribution and temporal evolution of the density of normal tissue, the neoplastic tissue growth and the excess H^+ ion concentration. Each of the model parameters has a corresponding biological interpretation, for instance, the growth rate of neoplastic tissue, the diffusion coefficient, the re-absorption rate and the destructive influence of H^+ ions in the healthy tissue.

The parameter is estimated by solving a minimization problem, in which the objective function is defined in order to compare both the real data and the numerical solution of the cancer invasion model. The real data can be obtained by, for example, fluorescence ratio imaging microscopy.

We apply a splitting strategy joint with the adaptive finite element method to numerically solve the model. The minimization problem (the inverse problem) is solved by using a gradient-based optimization method, in which the functional derivative is provided through an adjoint approach.

1. Introduction

Cancer is one of the diseases causing the most deaths in the world, despite the best efforts of medicine. Human and financial resources are devoted for cancer research, and on several occasions these efforts are successful [1–6].

Some comments on the importance of mathematical modeling in cancer can be found in the literature. In the work [4] the authors say "Cancer modelling has, over the years, grown immensely as one of the challenging topics involving applied mathematicians working with researchers active in the biological sciences. The motivation is not only scientific as in the industrial nations cancer has now moved from seventh to second place in the league table of fatal diseases, being surpassed only by cardiovascular diseases."

* Corresponding author. Tel.: +54 3514334051; fax: +54 3514334054.
E-mail addresses: aiquiroga@famaf.unc.edu.ar (A.A.I. Quiroga), dfernandez@famaf.unc.edu.ar (D. Fernández), torres@famaf.unc.edu.ar (G.A. Torres), turner@famaf.unc.edu.ar (C.V. Turner).

http://dx.doi.org/10.1016/j.amc.2015.08.038
0096-3003/

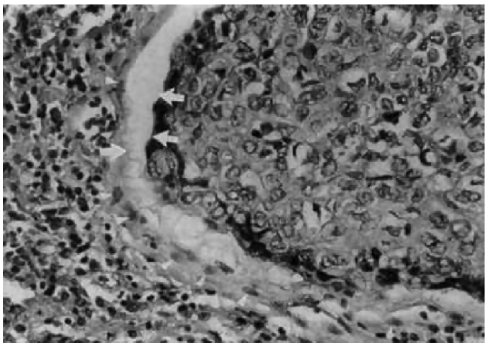

Fig. 1. Loss of normal cell layers in the tumor–host interface that facilitates tumor invasion [7, Fig. 4a].

We use the analysis proposed by Gatenby and Gawlinski in [7], which supports the acid-mediated invasion hypothesis. Therefore, it can be represented mathematically as a reaction–diffusion system which describes the spatial and temporal evolution of the tumor tissue, normal tissue, and excess H^+ ion concentration.

The model simulates a pH gradient extending from the tumor–host interface. The effect of biological parameters that control this transition is supported by experimental and clinical observations [8].

Some authors [7] model tumor invasion in order to find an underlying mechanism by which primary and metastatic cancers invade and destroy normal tissues. They do not attempt to model the genetic changes that lead to the transformation and seek to understand the causes of these changes. Likewise, they do not attempt to model the large-scale morphological aspects of tumor necrosis such as central necrosis. Instead, they concentrate on the interactions of microscopic scale populations that occur at the tumor–host interface, arguing that these processes influence the clinically significant manifestations of invasive cancer.

Moreover, in [7], the authors suppose that transformation-induced reversion of neoplastic tissue to primitive glycolytic metabolic pathways, with resultant increased acid production and the diffusion of that acid into surrounding healthy tissue, creates a peritumoral micro-environment in which the tumor cells survive and proliferate, while normal cells may not remain viable. The following temporal sequence would derive: (a) a high concentration of H^+ ions in tumors will diffuse chemically as a gradient to adjacent normal tissue, exposing these normal cells to an interstitial pH like in the tumor, (b) normal cells, immediately adjacent to the edge of the tumor, are unable to survive in this chronically acid environment, and (c) progressive loss of normal cell layers in the tumor–host interface facilitates tumor invasion, see Fig. 1. Key elements of this mechanism of tumor invasion include low pH due to primitive metabolism and reduced viability of normal tissue in an acidic environment.

This model depends only on a small number of cellular and sub-cellular parameters. The analysis of the equations shows that the model simulates a crossover from a benign tumor to a malignant invasive tumor when some combination of parameters turn over some threshold value.

We follow the PDE-based model by Gatenby and Gawlinski [7] (a coupled nonlinear system of partial differential equations), in a two-dimensional tissue and estimate one of its model parameters: the destructive influence of H^+ ions in the healthy tissue.

In this paper we propose a method to estimate the mentioned parameter via a PDE-constrained optimization problem. The objective function is defined as the difference between the real data and the numerical solution of the model in the Lebesgue measure. It is possible to get data of excess H^+ ion concentration [8] via fluorescence ratio imaging microscopy.

We solve the minimization problem using the trust-region-reflective method where the functional derivative is computed using the adjoint method.

The numerical solution of the model is obtained with a splitting strategy to divide the original problems in two simpler ones: (a) the first problem, consisting in a system of ordinary differential equations, corresponding to the reaction process, and (b) the second problem, consisting in a system of PDEs representing the diffusion process. This strategy allows a parallelization of the reaction problem. The PDE system is solved by the adaptive finite element method (AFEM).

This kind of minimization problem constitutes a particular application of the so-called inverse problems, which are being increasingly used in a broad number of fields in applied sciences. For instance, problems referred to structured population dynamics [9], computerized tomography and image reconstruction in medical imaging [10,11], and more specifically tumor growth [12–14], among many others.

This work follows the ideas in [15] where the space variable was in a one dimensional space. The extension of the model to two dimensional space allows us to approach the results to more realistic biological hypotheses. The differences of this work with respect to [15] are: (a) we take advantage of a more complex geometry in 2D instead of 1D, for the implementation of the finite element method (FEM); (b) we compute the *a posteriori* error estimation in order to use the adaptivity technique; (c) we use the splitting method to transform the original problem into two simpler problems, one of these is a linear problem, and the other one is nonlinear but parallelizable.

Regarding the novelty with existing literature, we cite two papers. Namely, Hogea et al. [13] model gliomas growth and their mechanical impact on the surrounding brain tissue. The model is a reaction–diffusion equation where the unknown is the local density of tumor cells. In our paper we have a coupled system of reaction–diffusion equations that considers competition terms.

The unknowns are tumor and health cell densities, and the excess H^+ ion concentration. The strategy in [13] to calculate the functional derivative is similar to ours, by using the adjoint approach. Additionally, we use adaptivity in order to control the discretization error.

On the other hand, Paruch and Majchrzak [16] solve an inverse problem where the PDE-constraint is the Pennes' equation. The minimization problem is solved by using evolutive and gradient-based algorithms. We shall stress that due to costly evaluation of our particular objective function, evolutionary algorithms are computationally more expensive that gradient-based methods.

The contents of this paper, which is organized into five sections, are as follows. Section 2 consists in some preliminaries about the model, the definition of variational form of the direct and adjoint problems, and the minimization problem. Section 3 deals with suitable numerical algorithms to solve the direct and adjoint problems. In particular, we use the splitting method and the adaptive finite element method with a computation of *a posteriori* error. In Section 4 we present numerical simulations of the retrieved parameter and the effectiveness of a parallel scheme. Section 5 presents the conclusions and some future work related to the contents of this paper.

Some words about our notation. We use $\langle \cdot, \cdot \rangle$ to denote the L^2 inner product (the space is always clear from the context) and we consider the sum of inner products for a Cartesian product of spaces. For a function $F : V \times U_{ad} \to \mathcal{Z}$ such that $(u, \delta) \mapsto F(u, \delta)$, we denote by $F'(u, \delta)$ the full Fréchet-derivative and by $\frac{\partial F}{\partial u}(u, \delta)$ and $\frac{\partial F}{\partial \delta}(u, \delta)$ the partial Fréchet-derivatives of F at (u, δ). For a linear operator $T : V \to \mathcal{Z}$ we denote $T^* : \mathcal{Z}^* \to V^*$ the adjoint operator of T.

2. Some preliminaries about the model

A mathematical model of the tumor–host interface based on the acid mediation hypothesis of tumor invasion due to [7] is given by the following system of partial differential equations (PDEs):

$$\begin{aligned}
\frac{\partial N_1}{\partial t} &= r_1 N_1 \left(1 - \frac{N_1}{K_1}\right) - d_1 L N_1, \\
\frac{\partial N_2}{\partial t} &= r_2 N_2 \left(1 - \frac{N_2}{K_2}\right) + \nabla \cdot \left(D_{N_2}\left(1 - \frac{N_1}{K_1}\right)\nabla N_2\right), \\
\frac{\partial L}{\partial t} &= r_3 N_2 - d_3 L + D_{N_3} \Delta L,
\end{aligned}$$

where the variables are in $\Omega \times [0, T]$, with $\Omega \subset \mathbb{R}^2$. These equations determine the spatial distribution and temporal evolution of three fields: N_1, the density of normal tissue; N_2, the density of neoplastic tissue; and L, the excess H^+ ion concentration. The units of N_1 and N_2 are cells/cm^3 and L is expressed as a molarity (M). The space $\mathbf{x}$ and time t are given in cm and seconds, respectively.

The biological meaning of each equation can be seen in [7], and the non-dimensional mathematical model is:

$$\begin{aligned}
\frac{\partial u_1}{\partial t} &= u_1(1 - u_1) - \delta_1 u_1 u_3, \\
\frac{\partial u_2}{\partial t} &= \rho_2 u_2(1 - u_2) + \nabla \cdot (D_2(1 - u_1)\nabla u_2), \\
\frac{\partial u_3}{\partial t} &= \delta_3(u_2 - u_3) + \Delta u_3,
\end{aligned} \tag{1}$$

where the four dimensionless quantities which parameterize the model are given by: $\delta_1 = d_1 r_3 K_2/(d_3 r_1)$, $\rho_2 = r_2/r_1$, $D_2 = D_{N_2}/D_{N_3}$ and $\delta_3 = d_3/r_1$.

The interaction parameters between different cells (healthy and tumor) and concentration of H^+ are difficult to measure experimentally. In particular, it is known that $\delta_1 < 1$ for noninvasive tumors and $\delta_1 > 1$ for frankly invasive malignant tumors. Hence, in this work we propose a technique to estimate the parameter δ_1.

The initial and boundary conditions considered for the non-dimensional system are:

$$\begin{aligned}
&u_1(\mathbf{x}, 0) = u_1^0(\mathbf{x}), \quad u_2(\mathbf{x}, 0) = u_2^0(\mathbf{x}), \quad u_3(\mathbf{x}, 0) = u_3^0(\mathbf{x}), \quad \forall \mathbf{x} \in \Omega, \\
&\frac{\partial u_1}{\partial n}(\mathbf{x}, t) = 0, \quad \frac{\partial u_2}{\partial n}(\mathbf{x}, t) = 0, \quad \frac{\partial u_3}{\partial n}(\mathbf{x}, t) = 0, \quad \forall \mathbf{x} \in \partial\Omega.
\end{aligned}$$

From now on, Eqs. (1) with the initial and boundary conditions will be referred to as the direct problem.

2.1. Variational form for the direct problem

Using the variational techniques for obtaining the weak solution of the direct problem [17–19], it can be written as $E(u, \delta_1) = 0$ where E: $V \times U_{ad} \to V^*$ such that

$$\begin{aligned}
\langle E(u, \delta_1), \lambda \rangle = &\int_0^T \int_\Omega \left(\frac{\partial u_1}{\partial t}\lambda_1 - u_1(1 - u_1)\lambda_1 + \delta_1 u_1 u_3 \lambda_1\right) d\mathbf{x}dt \\
&+ \int_0^T \int_\Omega \left(\frac{\partial u_2}{\partial t}\lambda_2 - \rho_2 u_2(1 - u_2)\lambda_2 + D_2(1 - u_1)\nabla u_2 \cdot \nabla \lambda_2\right) d\mathbf{x}dt
\end{aligned}$$

$$+\int_0^T\int_\Omega\left(\frac{\partial u_3}{\partial t}\lambda_3+\delta_3u_3\lambda_3-\delta_3u_2\lambda_3+\nabla u_3\cdot\nabla\lambda_3\right)d\mathbf{x}dt,$$
$$=\left\langle\frac{\partial u}{\partial t},\lambda\right\rangle-\langle F(u),\lambda\rangle-\langle A(u),\nabla\lambda\rangle,$$

where $V=W^3$, $u,\lambda\in V$, $u=(u_1,u_2,u_3)$, $\lambda=(\lambda_1,\lambda_2,\lambda_3)$ with

$$W=\left\{v: v\in L^2\big(0,T;H^1(\Omega)\big)\text{ and }\frac{\partial v}{\partial t}\in L^2(0,T;H^1(\Omega))\right\},$$

and $L^2(0,T;H^1(\Omega))=\left\{v: v(\cdot,t)\in H^1(\Omega)\text{ and }\|v(\cdot)\|_{H^1(\Omega)}\in L^2((0,T))\right\}$.

We use F: $V\to V^*$, A: $V\to V^*$ with

$$\begin{aligned}\langle F(u),\lambda\rangle &= \int_0^T\int_\Omega(u_1(1-u_1)-\delta_1u_1u_3)\lambda_1d\mathbf{x}dt\\ &\quad+\int_0^T\int_\Omega\rho_2u_2(1-u_2)\lambda_2d\mathbf{x}dt\\ &\quad+\int_0^T\int_\Omega\delta_3(u_2-u_3)\lambda_3d\mathbf{x}dt,\\ \langle A(u),\nabla\lambda\rangle &= -\int_0^T\int_\Omega D_2(1-u_1)\nabla u_2\cdot\nabla\lambda_2d\mathbf{x}dt-\int_0^T\int_\Omega\nabla u_3\cdot\nabla\lambda_3d\mathbf{x}dt.\end{aligned}\tag{2}$$

A weak solution $u\in V$ is a function that satisfies $\langle E(u,\delta_1),\lambda\rangle=0$ for all $\lambda\in V$.

2.2. Formulation of the minimization problem

As described above we propose to use an inverse problem technique in order to estimate δ_1. Function u represents the solution of the direct problem (the components of u are the state variables of the problem) for each choice of the parameter δ_1.

Let us assume that experimental information is available during the time interval $0\le t\le T$. Then, the inverse mathematical problem can be formulated as:

$$\begin{aligned}&\underset{(u,\delta_1)}{\text{minimize}} && J(u,\delta_1)\\ &\text{subject to} && E(u,\delta_1)=0,\\ &&& \delta_1\in U_{ad},\end{aligned}\tag{3}$$

where the objective functional $J: V\times U_{ad}\to\mathbb{R}$ is

$$J(u,\delta_1)=\frac{1}{2}\int_0^T\int_\Omega[u_3(\mathbf{x},t)-\hat{u}_3(\mathbf{x},t)]^2d\mathbf{x}dt,$$

with $u_3(\mathbf{x},t)$, the excess H^+ ion concentration obtained by solving the direct problem for a certain choice of δ_1 and $\hat{u}_3(\mathbf{x},t)$, the excess concentration measured experimentally (real data). One of the experimental methods to obtain values of $\hat{u}_3$ is by using fluorescence ratio imaging microscopy [8] (see Fig. 2).

The constraints are given by U_{ad}, the set of admissible values of δ_1 and E is the weak formulation of the direct problem.

From a physical point of view, the parameter δ_1 must lie in the interval $(0,\infty)$. However, according to the literature (for example, please refer to [7]), the parameter never reaches values greater than 12.5. Values of δ_1 greater than 12.5 implies a very fast destruction of the healthy cells.

We remark that, in general, there is a fundamental difference between the direct and the inverse problems. In fact, the latter is usually ill-posed in the sense of existence, uniqueness and stability of the solution. This inconvenient is often treated by using some regularization techniques [10,21,22]. In order to overcome instabilities we will use the Tikhonov regularization [23], thus we will consider:

$$J(u,\delta_1)=\frac{1}{2}\int_0^T\int_\Omega[u_3(\mathbf{x},t)-\hat{u}_3(\mathbf{x},t)]^2d\mathbf{x}dt+\frac{\epsilon}{2}(\delta_1-\delta_1^{\text{ref}})^2,\tag{4}$$

where $\epsilon>0$ and $\delta_1^{\text{ref}}\in U_{ad}$ are fixed parameters.

2.3. Formulation of the reduced and adjoint problems

In the following, we will consider the so-called reduced problem

$$\begin{aligned}&\underset{\delta_1}{\text{minimize}} && \tilde{J}(\delta_1)=J(u(\delta_1),\delta_1)\\ &\text{subject to} && \delta_1\in U_{ad},\end{aligned}\tag{5}$$

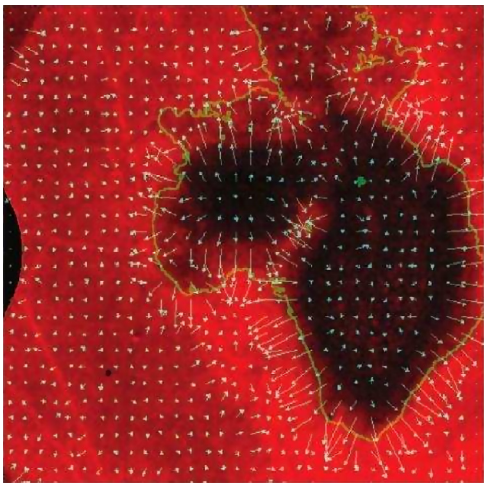

Fig. 2. A map of peritumoral H^+ flow using vectors generated from the pH distribution around the tumor [20, Fig. 4].

where $u(\delta_1)$ is given as the solution of $E(u(\delta_1), \delta_1) = 0$. In order to find a minimum of the continuously differentiable function $\tilde{f}$, it will be important to compute the derivative of this reduced objective function. Hence, we will show a procedure to obtain $\tilde{f}'$ by using the adjoint approach. According to the theory exposed in [24,25], the derivative of $\tilde{f}$ is given by

$$\tilde{f}'(\delta_1) = \frac{\partial J}{\partial \delta_1}(u(\delta_1), \delta_1) + \left(\frac{\partial E}{\partial \delta_1}(u(\delta_1), \delta_1)\right)^* \lambda, \tag{6}$$

where λ solves the so-called adjoint problem

$$\frac{\partial J}{\partial u}(u(\delta_1), \delta_1) + \left(\frac{\partial E}{\partial u}(u(\delta_1), \delta_1)\right)^* \lambda = 0. \tag{7}$$

Note that in order to obtain $\tilde{f}'(\delta_1)$ we need first to compute $u(\delta_1)$ by solving the direct problem, followed by the calculation of λ by solving the adjoint problem. For computing the second term of (6) it is not necessary to obtain the adjoint of $\frac{\partial E}{\partial \delta_1}(u(\delta_1), \delta_1)$ but just its action over λ.

Thus, the adjoint problem (7) consists in finding $\lambda \in V$ satisfying

$$\begin{aligned}
0 &= \left\langle \frac{\partial J}{\partial u}(u(\delta_1), \delta_1), \eta \right\rangle + \left\langle \frac{\partial E}{\partial u}(u(\delta_1), \delta_1)\eta, \lambda \right\rangle \\
&= \int_0^T \int_\Omega \left(-\frac{\partial \lambda_1}{\partial t}\eta_1 - \eta_1(1-2u_1)\lambda_1 + \delta_1 \eta_1 u_3 \lambda_1 - D_2 \eta_1 \nabla u_2 \cdot \nabla \lambda_2 \right) d\mathbf{x}dt \\
&\quad + \int_0^T \int_\Omega \left(-\frac{\partial \lambda_2}{\partial t}\eta_2 - \rho_2 \eta_2 (1-2u_2)\lambda_2 + D_2(1-u_1)\nabla \lambda_2 \cdot \nabla \eta_2 - \delta_3 \eta_2 \lambda_3 \right) d\mathbf{x}dt \\
&\quad + \int_0^T \int_\Omega \left(-\frac{\partial \lambda_3}{\partial t}\eta_3 + \delta_3 \eta_3 \lambda_3 + \nabla \lambda_3 \cdot \nabla \eta_3 + \delta_1 u_1 \eta_3 \lambda_1 \right) d\mathbf{x}dt \\
&\quad + \int_0^T \int_\Omega \eta_3 (u_3 - \hat{u}_3) d\mathbf{x}dt \\
&= \left\langle -\frac{\partial \lambda}{\partial t}, \eta \right\rangle + \left\langle G(\lambda), \eta \right\rangle + \left\langle B(\lambda), \nabla \eta \right\rangle,
\end{aligned} \tag{8}$$

where G and B are defined in a similar way as in (2), for all $\eta \in V$ and $\lambda(\mathbf{x}, T) = 0$. Then, since $\frac{\partial J}{\partial \delta_1} = \epsilon(\delta_1 - \delta_1^{\text{ref}})$, (6) can be written as

$$\tilde{f}'(\delta_1) = \frac{\partial J}{\partial \delta_1}(u(\delta_1), \delta_1) + \left(\frac{\partial E}{\partial \delta_1}(u(\delta_1), \delta_1)\right)^* \lambda = \epsilon(\delta_1 - \delta_1^{\text{ref}}) + \int_0^T \int_\Omega u_1 u_3 \lambda_1 d\mathbf{x}dt. \tag{9}$$

3. Designing an algorithm to solve the minimization problem

It is worth stressing that obtaining model parameters via minimization of the objective functional $\tilde{f}$ is in general an iterative process requiring the value of the derivative. To compute $\tilde{f}'$ we just solve two weak PDEs problems per iteration: the direct and

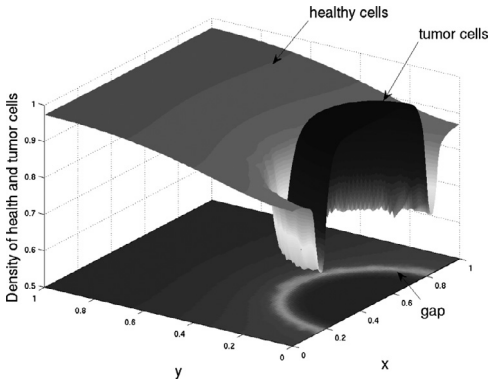

Fig. 3. In this 3D figure we plot the tumor and healthy cells density that are greater than 64% and its projection, for $\delta_1 = 12.5$ and $t = 10$. Note the gap between the healthy and tumor cells.

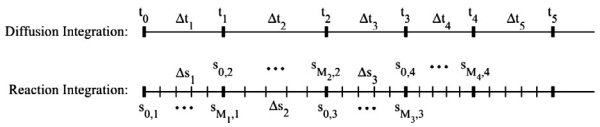

Fig. 4. Schematic picture of a temporal mesh for the splitting process [27, Section 2].

the adjoint problems. This method is much cheaper than the sensitivity approach [25] in which the direct problem is solved many times per iteration. We develop an implementation in MATLAB that solves the direct and adjoint problems. We use the splitting method in order to separate the direct problem in two new problems. The first one consists in a system of ordinary differential equations that contains the reaction terms of the original PDE. The second one is a PDE that contains the diffusion terms of the original PDE. The ODEs are solved by using the Runge–Kutta method (`ode45` MATLAB built-in function). Since we have an ODE system for each spatial point, its resolution can be parallelized accelerating the time execution. The PDE is solved by the adaptive finite element method. In the next subsections we will explain the splitting method and the adaptive procedure of the FEM. It is well-known [26] that gradient-based optimization algorithms require the evaluation of the gradient of the functional. The optimization problem is solved with a trust-region-reflective method, using the MATLAB built-in function `fmincon`.

For the direct problem, Fig. 3 shows the density of health cells, tumor cells and excess H^+ ion concentration at fixed time ($t = 10$) in terms of $\mathbf{x}$ variable.

3.1. Solving the direct problem

3.1.1. Splitting method

A multiscale operator splitting. We proceed like in [27, Section 2]. For the time discretization, we introduce a theoretical framework in which each component (the reaction component u^r and the diffusion component u^d) is solved exactly. We define a piecewise continuous approximate solution:

$$u(\mathbf{x}, t) = \frac{t_n - t}{\tau_n} u^{n-1}(\mathbf{x}) + \frac{t - t_{n-1}}{\tau_n} u^n(\mathbf{x})$$

for $t_{n-1} \le t \le t_n$, with the nodal values $u^n(\mathbf{x})$ obtained from the following procedure. We first discretize $[0, T]$ into $0 = t_0 < t_1 < \ldots < t_N = T$ with diffusion time step τ, $\tau = t_n - t_{n-1}$ for $n = 1, \ldots, N$. For each diffusion step, we choose a (small) time step $\tau_{s_n} = \tau / M_n$ where $M_n \in \mathbb{N}$, with $\tau_s = \max_{1 \le n \le N}\{\tau_{s_n}\}$, and the nodes $t_{n-1} = s_{0,n} < s_{1,n} < \ldots < s_{M_n,n} = t_n$ (see Fig. 4). We associate the time intervals $I_n = (t_{n-1}, t_n]$ and $I_{m,n} = (s_{m-1,n}, s_{m,n}]$ with these discretizations. Then, for $1 \le n < N$ do the following steps.

3.1.2. Algorithm

STEP 0: Given $u^{n-1}(\mathbf{x})$ and on the uniform mesh $\mathcal{T}$, do the following steps to compute $u^n(\mathbf{x})$.

STEP 1: Compute $u^r(\mathbf{x}, t)$ satisfying the reaction equation:

$$\left\langle \frac{\partial u^r}{\partial t}, \phi \right\rangle_{I_n} = \left\langle F(u^r), \phi \right\rangle_{I_n}$$
$$u^r(\mathbf{x}, t_{n-1}^+) = u^{n-1}(\mathbf{x})$$

for $s_{0,n} < t \le s_{M_n,n}$ and for all $\phi \in L^2(t_{n-1}, t_n; H^1(\Omega))$.

STEP 2: Compute $u^d(\mathbf{x}, t)$ satisfying the diffusion equation:

$$\left\langle \frac{\partial u^d}{\partial t}, \phi \right\rangle_{I_n} = \left\langle A(u^d), \phi \right\rangle_{I_n}$$

$$u^d(\mathbf{x}, t_{n-1}^+) = u^r(\mathbf{x}, t_n)$$

for $t_{n-1} < t \leq t_n$ and for all $\phi \in L^2(t_{n-1}, t_n; H^1(\Omega))$.

STEP 3: Set $u^n(\mathbf{x}) = u^d(\mathbf{x}, t_n)$,

where F and A are defined in (2). The equation in the Step 1 is a nonlinear, coupled system of first order ODE. In the Step 2 the equation is a second order PDE.

3.1.3. Adaptive FEM

The adaptive procedure for FEM consists in a four step loop: (a) solve the PDE using the FEM discretization, (b) estimate the *a posteriori* error of the discrete solution, (c) mark the elements to be refined according to the error size of the local *a posteriori* error, and (d) refine the marked elements keeping the mesh conformity (for more details see [28]).

Given a mesh $\mathcal{T}_n$ at time t_n, for all element $\mathcal{K} \in \mathcal{T}_n$, the element residual $R_{\mathcal{K}}(u^n)$ and the jump residual $J_S(u^n)$ are defined as:

$$R_{\mathcal{K}}(u^n) = \frac{u^n - u^{n-1}}{\tau} - \mathcal{A}(u^n), \quad \mathcal{K} \in \mathcal{T}_n \tag{10}$$

$$J_S(u^n) = -A(u^n) \cdot \nu^+ - A(u^n) \cdot \nu^-, \quad S \in \mathcal{S}_n \tag{11}$$

were $\mathcal{S}_n$ are the edges of $\mathcal{T}_n$, $\mathcal{A}$ is the right-hand side of (1) and the ν are the normals to the left and right of the corresponding edges.

We define the local error indicator $\eta(\mathcal{K})$ by

$$\eta(\mathcal{K})^2 = H_{\mathcal{K}}^2 \|R_{\mathcal{K}}(u^n)\|_{L^2(\mathcal{K})}^2 + \sum_{S \in \partial\mathcal{K}} H_S \|J_S(u^n)\|_{L^2(S)}^2,$$

were $H_{\mathcal{K}}$ is the diameter of $\mathcal{K}$ and H_S is the length of the edge S. If S is an edge of an element, then

$$\eta(S)^2 = H_S \|J_S(u^n)\|_{L^2(S)}^2.$$

The residual-type error estimator of Ω with respect to the mesh $\mathcal{T}_n$ is

$$\eta(\Omega)^2 = \sum_{\mathcal{K} \in \mathcal{T}_n} \eta(\mathcal{K})^2.$$

In this work we follow the technique proposed in [29], we use the `bulk` algorithm to mark (item (c)) and the `RedGreenBlue` algorithm to refine (item (d)). The bulk algorithm defines the set $\mathcal{E}$ of marked edges such that

$$\sum_{E \in \mathcal{E}} \eta(E)^2 \geq \theta \sum_{S \in \mathcal{S}_n} \eta(S)^2,$$

or it contains all the edges of marked elements $\mathcal{K} \in \mathcal{W} \subset \mathcal{T}_n$ that satisfy

$$\sum_{\mathcal{K} \in \mathcal{W}} \eta(\mathcal{K})^2 \geq \theta \sum_{\mathcal{K} \in \mathcal{T}_n} \eta(\mathcal{K})^2,$$

where $\mathcal{S}_n$ is the set of edges of $\mathcal{T}_n$ and $\theta \in [0, 1]$. In order to choose these edges we will use the following strategy: the local error, for edges or elements, is sorted in a descending form and are successively summed until the sum reaches the desired bound. Therefore those edges are chosen to be marked.

The RedGreenBlue can be briefly described as follows: elements with no marked edges are not refined, elements with one marked edge are refined green (divide the original triangle in two new triangles by using the midpoint of the marked edge and the opposite vertex), elements with two marked edges are refined blue (choose one of the marked edges and apply the green procedure, then apply green again on the triangle with the other marked edge) and elements with three marked edges are refined red (define a triangle with the midpoint of the edges).

Note that after the RedGreenBlue refinement for each $\mathcal{K} \in \mathcal{T}_{n-1}$, we have $\mathcal{T}_\ell|_{\mathcal{K}} = \{\tilde{\mathcal{K}} \in \mathcal{T}_\ell \mid \tilde{\mathcal{K}} \subset \mathcal{K}\}$ for all $\ell \geq n$.

3.1.4. Algorithm

STEP 0: Set an initial condition $u^0(\mathbf{x}) = u(\mathbf{x}, 0)$ on the coarse uniform mesh $\mathcal{T}_0$. Set $\varepsilon_{\text{TOL}} > 0$ and $n = 1$.

STEP 1: Given $u^{n-1}(\mathbf{x})$ and a mesh $\mathcal{T}_{n-1}$, compute $u^n(\mathbf{x})$ by using Algorithm 3.1.2.

STEP 2: Compute the *a posteriori* error $\eta(\Omega)$. If $\eta(\Omega) < \varepsilon_{\text{TOL}}$, set $\mathcal{T}_n = \mathcal{T}_{n-1}$ and either stop if $n = N$ or set $n = n + 1$ and go to STEP 1.

STEP 3: Mark and refine $\mathcal{T}_{n-1}$, and go to STEP 1.

In STEP 1, we compute u^r, the reaction component, by using the `ode45` MATLAB built-in function for each node of the current mesh, allowing a parallelization strategy. The diffusion component is solved by using FEM. In STEP 3, after the refinement process we obtain the values of u^{n-1} at the new nodes by using linear interpolation.

3.2. Solving the adjoint problem

In order to solve the adjoint problem we shall use FEM. The spatial discretization is the coarse mesh used for the initial mesh in the direct problem. We denote $\lambda^n(\mathbf{x}) = \lambda(\mathbf{x}, t_n)$ for $n = 0, \ldots, N$.

3.2.1. Algorithm

STEP 0: Set the final condition $\lambda^N(\mathbf{x}) = \lambda(\mathbf{x}, T) = 0$ on the initial mesh $\mathcal{T}_0$, and set $n = N$.

STEP 1: Given $\lambda^n(\mathbf{x})$, compute $\lambda^{n-1}(\mathbf{x})$ by solving an implicit Euler step in time and FEM in space:

$$\left\langle \frac{\lambda^n - \lambda^{n-1}}{\tau}, \eta \right\rangle = \left\langle G(\lambda^{n-1}), \eta \right\rangle + \left\langle B(\lambda^{n-1}), \nabla\eta \right\rangle,$$

where B and G are defined in (8).

STEP 2: Set $n = n - 1$ and go to STEP 1.

3.3. Solving the minimization problem

The `fmincon` MATLAB built-in function was used to solve the minimization problem. The chosen algorithm in the `fmincon` function was the trust-region-reflective method, where the derivative of the objective function $\tilde{J}$ was computed according to 9.

3.3.1. Algorithm

The method we will use for minimizing the functional $\tilde{J}$ can be summarized as follows:

STEP 0: Give an initial guess δ_1^0 for the parameter.

STEP 1: Call the `fmincon` function and obtain the solution δ_1^*, providing the value of the objective function $\tilde{J}(\delta)$ and its derivative $\tilde{J}'(\delta)$ according to (5) and (9), respectively.

In order to compute $\tilde{J}(\delta)$ and $\tilde{J}'(\delta)$ is necessary to solve the direct and adjoint problems.

4. Numerical experiments

The goal of this section is to test and evaluate the performance of an adjoint-based optimization method, by executing some numerical simulations of Algorithm 3.3.1 for some test cases. The experiments were run in MATLAB, in a PC running Linux, with four quad-cores of 2.4 GHz.

In our case we will consider the space domain $\Omega = [0, 1] \times [0, 1]$, the time domain $[0, 10]$ (*i.e.*, $T = 10$), and the following model parameters: $\rho_2 = 1$, $D_2 = 4 \times 10^{-5}$ and $\delta_3 = 1$.

In a real case, we need experimental data provided by measurements. That is, a series of values $\hat{u}_3(\mathbf{x}, t)$ should be provided at a coarse space mesh $\mathcal{T}_0$ and at a time mesh $0 = t_0 < t_1 < \ldots < t_N = T$.

Numerical experiments are performed with $\hat{u}_3(\mathbf{x}, t)$ generated via the direct problem for some $\hat{\delta}_1$ in a coarse mesh $\mathcal{T}_0$ having 512 triangular elements covering Ω, and $t_i = t_{i-1} + 0.1$, $i = 1, \ldots, 100$. Thus, the evaluation of the functional defined in (5) is performed by integrating over this spatial and time discretization. In order to get a representative value of the objective functional without regularization, we set $c_0 = \tilde{J}(\delta_1^0)$ choosing $\epsilon = 0$. For an appropriate scaling of the regularization term we take the value of the Tikhonov regularization parameter as $\epsilon = 10^{-5} c_0$, and the reference point is $\delta_1^{\text{ref}} = 0$ to avoid the function flatness for large values of δ_1 as observed in the experiments. For numerical considerations, we will work with the scaled functional $\tilde{J}/c_0$.

Regarding Algorithm 3.1.4 we have used the following parameters: $\varepsilon_{\text{TOL}} = 10^{-5}$ and $\theta = 1/2$. In the STEP 1, we have to call Algorithm 3.1.2 to go forward in time. This is done solving a system of ODEs for each node of the current mesh. A parallel strategy (each processor solves a system of ODEs for one node) is the best and natural option to reduce time execution. For example, Fig. 5(a) shows how many seconds takes to solve the direct problem, and Fig. 5(b) shows the speed-up. This parallel strategy is very useful since the optimization solver could call Algorithm 3.1.4 many times.

The time step τ in Algorithm 3.2.1 is set to 0.1. Regarding Algorithm 3.3.1 we have set the feasible set $U_{ad} = [0, 20]$ in the minimization problem (5). Besides that, the method used in the `fmincon` routine (STEP 1) is the trust-region-reflective method [30,31], where the option `GradObj` is on (the gradient of the objective function must be supplied) and the maximum of function evaluations of $\tilde{J}$ is 100. If we use an algorithm where the gradient is estimated by finite differences, the procedure will become computationally more expensive due to costly evaluation of the objective function. That is the reason for which we compute the exact derivative of the functional using the adjoint method.

Let us consider an optimization problem that consists in minimizing the functional defined in (5) for different $\hat{u}_3$ corresponding to $\hat{\delta}_1 = 4,\ 12.5,\ 16$. The choice of these values is associated with different behaviors of tumor invasion, according to [7]. The idea of these test cases is to investigate how close the original value of the parameter can be retrieved (even in the presence of noise), and how efficiently these computations can be done.

Fig. 6(a) shows the graph of the functional $\tilde{J}$ defined in (5) takes with respect to δ_1, for $\hat{u}_3$ generated with $\hat{\delta}_1 = 12.5$. It is worth mentioning that, even when we do not know in advance if the optimization problem has a unique solution, $\tilde{J}$ looks convex with respect to δ_1.

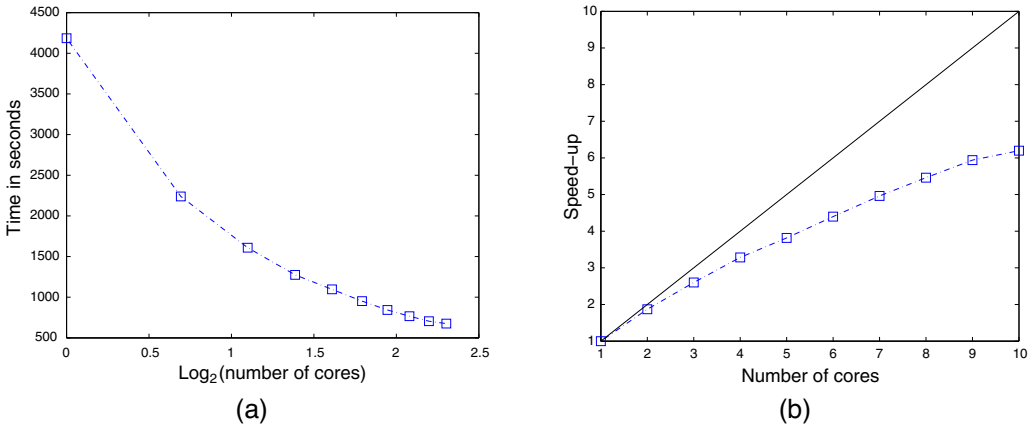

Fig. 5. (a) Time in seconds of the direct problem execution, (b) graph of the speed-up for solving the direct problem.

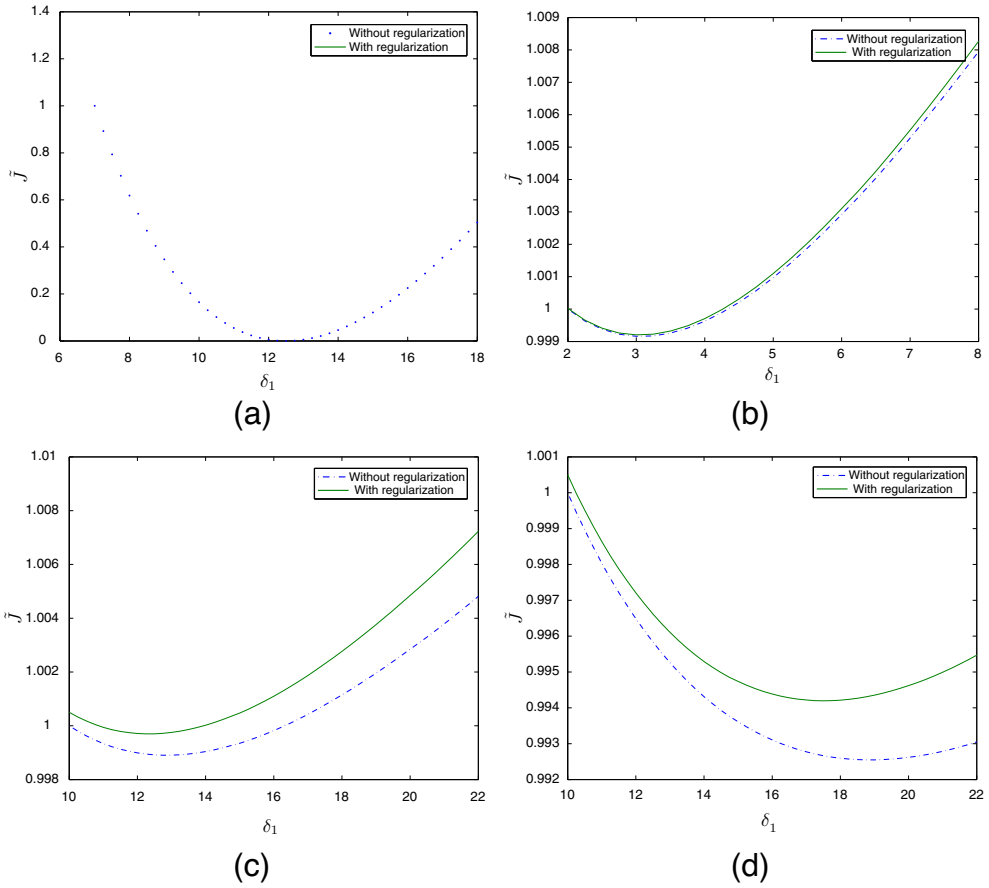

Fig. 6. Graph of functional $\tilde{J}$ with and without regularization for $\hat{u}_3$ generated with some $\hat{\delta}_1$ and error σ. (a) $\hat{\delta}_1 = 12.5$, $\sigma = 0$. (b) $\hat{\delta}_1 = 4$, $\sigma = 0.1$. (c) $\hat{\delta}_1 = 12.5$, $\sigma = 0.15$. (d) $\hat{\delta}_1 = 16$, $\sigma = 0.2$.

We have run Algorithm 3.3.1, with $\tilde{J}$ without regularization, for each of the chosen values of $\hat{\delta}_1$ taking the initial condition δ_1^0 randomly. It is worth stressing that the retrieved parameter is obtained very accurately, independently of the value of δ_1^0. Averaging the different solutions, obtained for different choices of δ_1^0, and taking the standard deviation of all of these experiments, we get Table 1. Thus, in the next experiment we will consider a fixed value for δ_1^0.

It is well-known that the presence of noise in the data may imply the appearance of strong numerical instabilities in the solution of an inverse problem [32]. As it is well-known, measurements are often affected by perturbations, usually random

Table 1
Experiments for randomly initial data δ_1^0.

$\hat{\delta}_1$	$\bar{\delta}_1$	S
4	4.2666	$\pm 7.0640 \times 10^{-3}$
12.5	12.4937	$\pm 7.1875 \times 10^{-4}$
16	16.6246	$\pm 1.8826 \times 10^{-5}$

Table 2
Experiments for $\hat{\delta}_1 = 4$.

σ	$\bar{\delta}_1$	S	e_{δ_1}
0.1000	3.2500	±1.0000	0.1875
0.1500	3.9167	±1.0104	0.0208
0.2000	3.3333	±1.1273	0.1667

Table 3
Experiments for $\hat{\delta}_1 = 12.5$.

σ	$\bar{\delta}_1$	S	e_{δ_1}
0.1000	12.2500	±2.1360	0.0200
0.1500	13.5833	±3.6257	0.0867
0.2000	13.5000	±2.8831	0.0800

Table 4
Experiments for $\hat{\delta}_1 = 16$.

σ	$\bar{\delta}_1$	S	e_{δ_1}
0.1000	15.3333	± 4.2303	0.0417
0.1500	14.8333	± 2.0966	0.0729
0.2000	16.8333	± 3.7109	0.0521

ones. Then we perform numerical experiments where $\hat{u}_3$ is perturbed by using Gaussian random noise with zero mean and standard deviation $\sigma = 0.1,\ 0.15,\ 0.2$. Considering $\delta_1^0 = 8$ in all cases, Tables 2–4 show the average $\bar{\delta}_1$ (over 10 values of δ_1^*), the standard deviation S and the relative error $e_{\delta_1} = |\bar{\delta}_1 - \hat{\delta}_1|/|\hat{\delta}_1|$ for each value of σ.

5. Final conclusions and future work

In this paper we have solved a parameter estimation problem following the model proposed by [7] in a two-dimensional space. The inverse problem is formulated as an optimization problem in order to find the parameter δ_1 (the destructive influence of H^+ ions in the healthy tissue).

The direct problem was solved by the splitting technique together with adaptive finite element method, for the purpose of controlling the numerical error and defining a parallel strategy. A gradient-based method was used to solve the optimization problem. The derivative of the objective functional was computed using the solution of the adjoint problem.

The experiments were run in MATLAB recovering several values of the parameter δ_1 representing different scenarios. Also, a stability analysis was performed using random noise to simulate perturbations in the experimental data.

We consider that the results are accurately enough. In most cases the parameters are retrieved with a relative error less than 20%.

As a future work we propose to consider the possibility to find optimal parameters related to therapeutic procedures like in [33,34].

Acknowledgments

We appreciate the courtesy of Sebastián Pauletti, from IMAL, Santa Fe, Argentina, who strongly contributed with information above splitting method. We also thank the referees for their valuable suggestions.

The work of the authors was partially supported by grants from CONICET (PIP 11220110100050), SECyT-UNC (307201101013332CB, 30720130100604CB), PICT-FONCyT.

References

[1] J. Adam, A simplified mathematical model of tumor growth, Math. Biosci. 81 (2) (1986) 229–244.

[2] J. Adam, N. Bellomo, A Survey of Models for Tumor Immune Systems Dynamics, Modeling and Simulation in Science, Engineering & Technology, Birkhäuser, 1997.
[3] N. Bellomo, M. Chaplain, E. De Angelis, Selected Topics on Cancer Modeling—Genesis–Evolution–Immune Competition–Therapy, Birkhäuser, Boston, 2009.
[4] N. Bellomo, N. Li, P. Maini, On the foundations of cancer modelling: selected topics, speculations, and perspectives, Math. Models Methods Appl. Sci. 18 (04) (2008) 593–646.
[5] H.M. Byrne, Dissecting cancer through mathematics: from the cell to the animal model, Nat. Rev. Cancer 10 (3) (2010) 221–230.
[6] N. Bellomo, L. Preziosi, Modelling and mathematical problems related to tumor evolution and its interaction with the immune system, Math. Comput. Model. 32 (3) (2000) 413–452.
[7] R.A. Gatenby, E.T. Gawlinski, A reaction–diffusion model of cancer invasion, Cancer Res. 56 (24) (1996) 5745–5753.
[8] G.R. Martin, R.K. Jain, Noninvasive measurement of interstitial pH profiles in normal and neoplastic tissue using fluorescence ratio imaging microscopy, Cancer Res. 54 (21) (1994) 5670–5674.
[9] B. Perthame, J. Zubelli, On the inverse problem for a size-structured population model, Inverse Probl. 23 (3) (2007) 1037–1052.
[10] K. van den Doel, U.M. Ascher, D.K. Pai, Source localization in electromyography using the inverse potential problem, Inverse Probl. 27 (2) (2011) 025008.
[11] J. Zubelli, R. Marabini, C. Sorzano, G. Herman, Three-dimensional reconstruction by Chahine's method from electron microscopic projections corrupted by instrumental aberrations, Inverse Probl. 19 (4) (2003) 933–949.
[12] J. Agnelli, A. Barrea, C. Turner, Tumor location and parameter estimation by thermography, Math. Comput. Model. 53 (2011) 1527–1534.
[13] C. Hogea, C. Davatzikos, G. Biros, An image-driven parameter estimation problem for a reaction–diffusion glioma growth model with mass effects, J. Math. Biol. 56 (6) (2008) 793–825.
[14] D.A. Knopoff, D.R. Fernández, G.A. Torres, C.V. Turner, Adjoint method for a tumor growth PDE-constrained optimization problem, Comput. Math. Appl. 66 (6) (2013) 1104–1119.
[15] A.A.I. Quiroga, D.R. Fernández, G.A. Torres, C.V. Turner, Adjoint method for a tumor invasion PDE-constrained optimization problem using FEM, arXiv:1405.4912.
[16] M. Paruch, E. Majchrzak, Identification of tumor region parameters using evolutionary algorithm and multiple reciprocity boundary element method, Eng. Appl. Artif. Intell. 20 (5) (2007) 647–655.
[17] O.A. Ladyzhenskaia, V.A. Solonnikov, Linear and Quasi-linear Equations of Parabolic Type, vol. 23, American Mathematical Society, 1988.
[18] D. Kinderlehrer, G. Stampacchia, An Introduction to Variational Inequalities and Their Applications, Society for Industrial and Applied Mathematics, 1987.
[19] L.C. Evans, Partial Differential Equations, American Mathematical Society, 1998.
[20] R.A. Gatenby, E.T. Gawlinski, A.F. Gmitro, B. Kaylor, R.J. Gillies, Acid-mediated tumor invasion: a multidisciplinary study, Cancer Res. 66 (10) (2006) 5216–5223.
[21] H.W. Engl, M. Hanke, A. Neubauer, Regularization of Inverse Problems, vol. 375, Kluwer Academic Pub, 1996.
[22] A. Kirsch, An Introduction to the Mathematical Theory of Inverse Problems, 120, Springer Science+ Business Media, 2011.
[23] H.W. Engl, C. Flamm, P. Kügler, J. Lu, S. Müller, P. Schuster, Inverse problems in systems biology, Inverse Probl. 25 (12) (2009) 123014.
[24] C. Brandenburg, F. Lindemann, M. Ulbrich, S. Ulbrich, A continuous adjoint approach to shape optimization for Navier Stokes flow, Optimal Control of Coupled Systems of Partial Differential Equations, Springer, 2009, pp. 35–56.
[25] M. Hinze, Optimization with PDE Constraints, vol. 23, Springer, 2009.
[26] J. Nocedal, S.J. Wright, Numerical Optimization, Springer Science+ Business Media, 2006.
[27] D. Estep, V. Ginting, D. Ropp, J.N. Shadid, S. Tavener, An a posteriori–a priori analysis of multiscale operator splitting, SIAM J. Numer. Anal. 46 (3) (2008) 1116–1146.
[28] R.H. Nochetto, K.G. Siebert, A. Veeser, Theory of adaptive finite element methods: an introduction, Multiscale, Nonlinear and Adaptive Approximation, Springer, 2009, pp. 409–542.
[29] A. Byfut, J. Gedicke, D. Günther, J. Reininghaus, S. Wiedemann, et al., FFW Documentation, Humboldt University of Berlin, Germany.
[30] T.F. Coleman, Y. Li, A reflective Newton method for minimizing a quadratic function subject to bounds on some of the variables, SIAM J. Optim. 6 (4) (1996) 1040–1058.
[31] MATLAB. http://www.mathworks.com/, 2013.
[32] M. Bertero, M. Piana, Inverse problems in biomedical imaging: modeling and methods of solution, Complex Systems in Biomedicine, Springer, 2006, pp. 1–33.
[33] J.B. McGILLEN, N.K. Martin, I.F. Robey, E.A. Gaffney, P.K. Maini, Applications of mathematical analysis to tumour acidity modelling, RIMS Kokyuroku Bessatsu 31 (2012) 31–59.
[34] N. Martin, I. Robey, E. Gaffney, R. Gillies, R. Gatenby, P. Maini, Predicting the safety and efficacy of buffer therapy to raise tumour PHE: an integrative modelling study, Br. J. Cancer 106 (7) (2012) 1280–1287.